JMEPEG (2012) 21:973–976
DOI: 10.1007/s11665-011-9965-5

1059-9495/$19.00

Microstructure Evolution and Mechanical Properties of As-Cast Pb-Mg-Al Alloys

Y.H. Duan, Y. Sun, M.J. Peng, Zh.Zh. Guo, and P.X. Zhu

(Submitted July 5, 2010; in revised form April 18, 2011)

In this study, two new types of Pb-Mg-Al alloys with high tensile strength and hardness were prepared by casting under the molten salt. The microstructure and morphology of the Pb-Mg-Al alloys were investigated through x-ray diffraction and scanning electron microscope analysis. Mechanical properties of the alloys were compared with those of the pure Pb and its alloys, and the results indicate that the tensile strength and hardness increase, respectively, up to 300 MPa and 156 HB with the 10 wt.% addition of Al. The fractographic examinations indicate that the fracture model of Pb-Mg-Al alloys changes from mixed intergranular-transgranular to the intergranular quasi-cleavage with the increase in Al content.

Keywords fracture, microstructure, Pb-Mg-Al alloy, strengthening mechanism

1. Introduction

Lead and its alloys have frequently been used in a variety of industrial applications, such as grid electrode, x-ray shielding materials, lead-acid batteries, etc. Most of the traditional lead alloys are the solid solution composite materials reinforced by second phase particle (Ref 1-6). However, they are still unable to meet the requirements of structural materials. In recent years, researchers paid little attention to the Pb-based Pb-Mg-Al alloy, but they focused more on the Mg-based alloys with small amounts of Pb or Al relatively. Cacciamani et al. (Ref 7) have researched the thermodynamic properties of Pb-Mg alloy. Wang et al. (Ref 8) have reported the effects of heat treatment on organizations and performance of Mg-Pb binary as-cast Mg-based alloy, and the effect of rare earths neodymium on the above alloy. Wang et al. (Ref 9) have studied the microstructures, mechanical properties, and compressive creep behaviors of as-cast Mg-5%Sn-(0-1.0)%Pb alloys.

Therefore, in order to obtain a new type of lead matrix alloy with high tensile strength and hardness in this investigation, Pb-Mg-Al alloys were prepared. A systematic investigation is necessary to analyze the microstructure and understand the tensile behavior of Pb-Mg-Al alloys.

This study is devoted to investigate the tensile properties of the newly developed Pb-Mg-Al alloys at room temperature compared with the traditional Pb alloys, such as Pb-Ca and Pb-Sb alloys, and finally obtain the strengthening mechanism of Pb-Mg-Al alloys. The microstructure is also thoroughly investigated, in addition, to determine the effect of Al addition on promoting the properties of Pb-Mg alloys.

Y.H. Duan, Y. Sun, M.J. Peng, Zh.Zh. Guo, and **P.X. Zhu**, Faculty of Material Science and Technology, Key Lab of Advanced Materials of Yunnan Province, Kunming University of Science and Technology, Yunnan, Kunming, People's Republic of China. Contact e-mail: 19508150@sina.com.cn.

2. Experimental

In this study, the Pb-Mg-Al alloys with the compositions (wt.%) were prepared by induction melting with Pb, Mg, and Al (purity 99.99) as raw materials in the graphite crucible under the melting salt composed by 46% $MgCl_2$, 44% KCl, 7% NaCl, and 3% MgO (wt.%). The chemical compositions of the two Pb-Mg-Al alloys were constituted by 38% Mg, 57% Pb, and 5% Al for alloy 1, and 36% Mg, 54% Pb and 10% Al (wt.%) for alloy 2, with the mass ratio of Mg and Pb being 2/3. The molten alloy in crucible was chill cast in a steel model to form cylindrical ingots of 15 mm in diameter. A cooling rate of 8-10 °C/s was achieved, so as to create the fine microstructure typically found in small alloy joints in microelectronic packages. To observe the microstructure of the two as-cast Pb-based alloys, the as-cast specimens were annealed at 200 °C for 1 h, polished with synthetic diamond paste after grinding, and cleaned with alcohol lastly without etching treatment. The general morphologies of as-cast specimens were examined by scanning electron microscope (SEM). Energy dispersive x-ray analysis (EDX) was employed to determine the chemical composition of the alloys. The crystal phases were analyzed by x-ray diffractometer (XRD) measured using Bruker D8 Advance Cu K_α radiations (λ = 1.5406 Å) in the range of 10-100 at 30 kV and 30 mA. The hardness tests were determined using HB-3000 type Brinell's machine and HX-1 type Vickers pyramid hardness machine. The Brinell hardness number of each alloy was obtained from the average value of six different points on testing surface, and the Vickers hardness figure was obtained from the average value of eight different points on each phases. The tensile tests were performed on the alloys by MTS type machine with experimental error less than ±3% (MTS 810 Teststar). The tests were carried out at constant temperature of 25 °C. In order to elucidate the macroscopic deformation mechanisms of the alloys, fracture surface of alloys after tensile tests were analyzed using SEM.

3. Results and Discussion

3.1 Microstructure

X-ray diffraction patterns of all the alloys are shown in Fig. 1. From the XRD patterns of alloys 1 and 2, four different phases, namely, α-Mg, β-Pb, Mg_2Pb, and $Mg_{17}Al_{12}$, are detected in the Pb-Mg-Al alloys. The main sharp diffraction peaks in Fig. 1 are identified as a mixture of hexagonal α-Mg, face-centered cubic β-Pb, body-centered cubic Mg_2Pb and $Mg_{17}Al_{12}$ phases. Figure 1 displays that diffraction intensities of α-Mg and Mg_2Pb compounds decreased gradually with increasing Al content, whereas β-Pb and $Mg_{17}Al_{12}$ precipitate phases increased continuously. It indicates that the addition of Al is able to control effectively a volume fraction of the brittle Mg_2Pb (Ref 10).

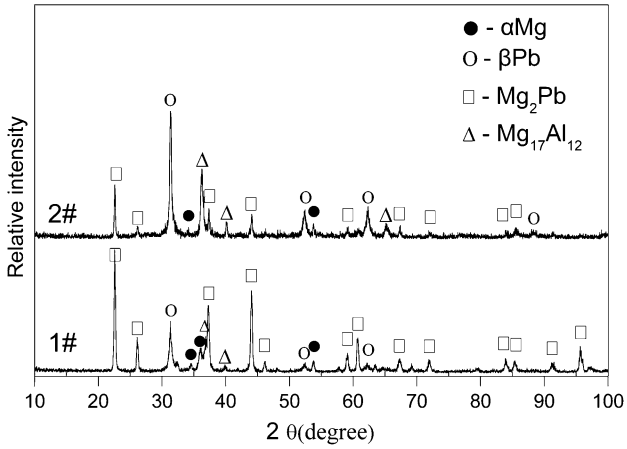

Fig. 1 X-ray diffraction patterns of alloys

Two reactions that take place among Pb, Mg, and Al in the Pb-Mg-Al alloys are as follows:

$$Pb + 2Mg = Mg_2Pb \quad \text{(Eq 1)}$$

$$17Mg + 12Al = Mg_{17}Al_{12} \quad \text{(Eq 2)}$$

The Gibbs free energies (ΔG^{θ}) of reactions (1) and (2), are −44.87 and −625.34 kJ/mol, respectively, having also been calculated previously by the thermodynamic data (Ref 11, 12). The result indicates that the Gibbs free energies of the two reactions are negative, and so the formations of the Mg_2Pb and $Mg_{17}Al_{12}$ phases directly from the reactions among Pb, Mg, and Al are advantageous in thermodynamics.

In order to distinguish the characteristics of Mg_2Pb and $Mg_{17}Al_{12}$, the backscattered electron scanning microscopy was employed to further examine the microstructure, as shown in Fig. 2. From a ternary Mg-Al-Pb phase diagram (Ref 13), previous XRD patterns and EDX analysis, it is clear that the white microscale structure is of Mg_2Pb phase which is skeleton in alloy 1 and lath in alloy 2. The SEM image, shown in Fig. 2(a), obtained from alloy 1 reveals that the skeleton Mg_2Pb phases are distributed homogeneously in the matrix. Furthermore, the volume fraction of the Mg_2Pb phases is estimated to be ∼45%. The magnified SEM micrographs from Fig. 2(a), Fig. 2(b) reveal a typical ultrafine eutectic $Mg_{17}Al_{12}$ and β-Pb with an acicular size of 1-2 μm. The SEM image, Fig. 2(c), obtained from alloy 2 shows that the volume fraction of the

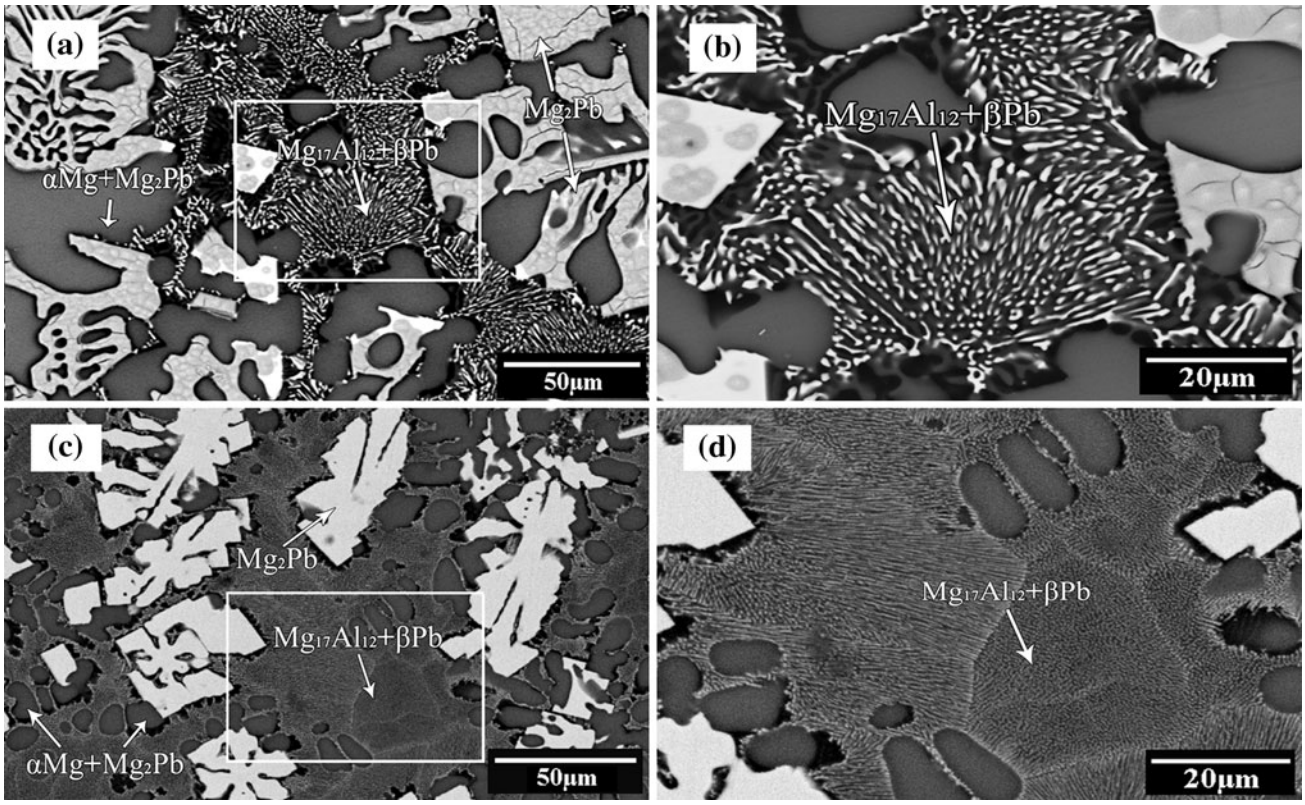

Fig. 2 SEM-BSE micrographs of the alloys 1 and 2: (a) the morphologies and phases in the alloy 1; (b) a magnified view of white boundary marked region in (a); (c) the morphologies and phases in the alloy 2; (d) a magnified view of white boundary marked region in (c)

Mg_2Pb phases is estimated to be ~41%. One can find from Fig. 2(c) and Fig. 2(d) that the shape of Mg_2Pb gradually degenerates to lath, and the size of eutectic $Mg_{17}Al_{12}$ and β-Pb decreases to <0.5 μm with Al content increasing. In addition, the size of eutectic, namely, α-Mg and Mg_2Pb, also decreases with the Al content increasing. In contrast, there is clear difference in volume fraction values with increasing eutectic $Mg_{17}Al_{12}$ and β-Pb and decreasing α-Mg and Mg_2Pb . Hence, it is feasible to suggest that Al plays an important role in governing the growth of Mg_2Pb and eutectic α-Mg and Mg_2Pb because of the appearance of a large number of ultrafine acicular $Mg_{17}Al_{12}$ and β-Pb phases.

3.2 Mechanical Properties

3.2.1 Tensile and Hardness Properties. Table 1 shows the mechanical properties of alloy 1 and 2 compared with pure Pb and its alloys, obtained from tensile and hardness tests at room temperature. In order to obtain the effect of Al content on the tensile strength and Brinell hardness of Pb-Mg-Al alloys, a typical Pb-40Mg alloy without Al was prepared by casting. While comparing, with respect to Pb-40Mg alloy, with the values of tensile strength and Brinell hardness at room temperature, 103 MPa and 71 HB, respectively, the alloy 1 fabricated by the present experimental procedure has higher value of 228 MPa for tensile strength and 117 HB for Brinell hardness. With Al content increasing to 10 wt.%, the values of the corresponding mechanical properties increase even up to 300 MPa and 156 HB. These values are higher than that of pure Pb and its alloys. As shown in Table 1, pure Pb without any addition has the highest %elongation to failure value, which is about 30-50. The content of 40 wt.% Mg addition exhibits 0.23% of elongation to failure, which drops rapidly from the initial value of 30-50%. The compositions with 5 wt.% Al reinforcement reveal a relatively higher % of elongation. At 10 wt.% of Al reinforcement shows an obviously higher %elongation values compared with Pb-40Mg alloy. It is found that the larger the wt.% of Al addition, the higher the tensile strength and the strain that are experienced before failure. However, the % of elongation to failure of Pb-Mg-Al alloys is lower than pure Pb, Pb-Ca, Pb-Sb, and Sn-Pb alloys.

The hardness of various phases in samples and the relationship of microstructure and performance can be obtained and analyzed through the microhardness test. Table 2 lists the Vickers hardness figure of each phase in the Pb-Mg-Al alloys at room temperature. From Table 2, the Vickers hardness figures of eutectic α-Mg and Mg_2Pb are about 57.6 HV in both alloys 1 and 2. However, with Al content increasing, the values of Mg_2Pb phase and acicular $Mg_{17}Al_{12}$ and β-Pb phase increase up to 100.4 and 104 HV from 98.6 and 96 HV, respectively. Pb-Mg-Al alloys with higher wt.% Al addition have exhibited higher hardness values owing to the presence of the homogeneous distribution and size of Al intermetallic in the alloys. It reveals that the addition of Al can control the crystal growth and cause crystal refinement resulting in the enhancement of tensile strength and hardness.

On the one hand, the electronic structure of intermetallic Mg_2Pb have been calculated and analyzed by density functional theory (DFT) (Ref 17), the results show that there are shared charges with a strong delocalization between Mg and Pb atoms in Mg_2Pb crystal, so as to form covalent bonds. The bonding of covalent bond is higher than that of metal and ionic bonds, and the covalent bond can enhance the strength and hardness owing to its high Peierls-Nabarro stress and directionality. Moreover, because $Mg_{17}Al_{12}$ is also an intermetallic compound with complicated crystal structure and low symmetry, it leads to a decrease in the mobility of atoms and dislocations, improving further the strength and the hardness of Pb-Mg-Al alloys. Moreover, the calculated Young's modulus and shear modulus values are 68.6 and 27.9 GPa for Mg_2Pb, and 117.1 and 51.3 GPa for $Mg_{17}Al_{12}$, which are far larger than the experimental results of 16.5 and 5.8 GPa for Pb. It is believed that the intermetallics in Pb-Mg-Al alloys are beneficial to the strengthening of the alloys.

The lower elongations of these two experimental Pb-Mg-Al alloys are also affected mainly by the two kinds of intermetallic compounds, namely, Mg_2Pb and $Mg_{17}Al_{12}$. It is difficult to produce deformation through the movement of the dislocation due to their higher Peierls-Nabarro stress and directionality. The Poisson's ratio ν is generally 1/3 for ductile materials, whereas it is $<1/3$ for brittle materials (Ref 18). Poisson's ratios ν of Mg_2Pb and $Mg_{17}Al_{12}$ are about 0.23 and 0.14, respectively; since both of them are $<1/3$, Mg_2Pb and $Mg_{17}Al_{12}$ are brittle. As a result, the elongation values of Pb-Mg-Al alloys are lower than those of pure Pb and its alloys.

On the other hand, the addition of Al refines the grain size of the eutectics ($Mg_{17}Al_{12}$ and β-Pb, α-Mg and Mg_2Pb) and increases the strength and hardness of the Pb-Mg-Al alloys.

3.2.2 Facture Morphology. Figure 3(a) and 3(b) shows SEM micrographs obtained from the fracture surfaces of the experimental Pb-Mg-Al alloys. The base alloys usually fracture in the form of cleavage and (or) intergranular at room temperature, in which the fractures of alloys are dependent on their relative strength to each other. The SEM fractography of the alloy 1 in Fig. 3(a) reveals a mixed intergranular-transgranular fracture morphology indicating brittle deformation. In contrast, SEM micrograph of the alloy 2 in Fig. 3(b)

Table 1 The contrast of mechanical properties (tensile strength (MPa), Brinell hardness (HB), and elongation (%)) at room temperature among Pb and its alloys, alloys 1 and 2

Alloys	Tensile strength	Brinell hardness	Elongation	Ref.
Pb-38Mg-5Al	228	117	0.48	This work
Pb-36Mg-10Al	300	156	0.65	This work
Pb-40Mg	103	71	0.23	This work
Pure Pb	10-20	4-9	30-50	Ref 14
Pb-8Sb	17-29	4-13	40	Ref 14
Pb-0.4Ca-1Sn	29.8	13.7	28	Ref 5
Pb-0.4Ca-1Sn	49	···	10	Ref 15
Sn-37Pb	52-66	···	31-41	Ref 16

Table 2 The Vickers hardness figure of each phase in alloys 1 and 2 at room temperature

Phase	Vickers hardness (HV)
Eutectic α-Mg and Mg_2Pb in alloy 1	57.6
Eutectic α-Mg and Mg_2Pb in alloy 2	57.7
Skeleton Mg_2Pb in alloy 1	98.6
Lath Mg_2Pb in alloy 2	100.4
Acicular $Mg_{17}Al_{12}$ and β-Pb in alloy 1	96
Acicular $Mg_{17}Al_{12}$ and β-Pb in alloy 2	104

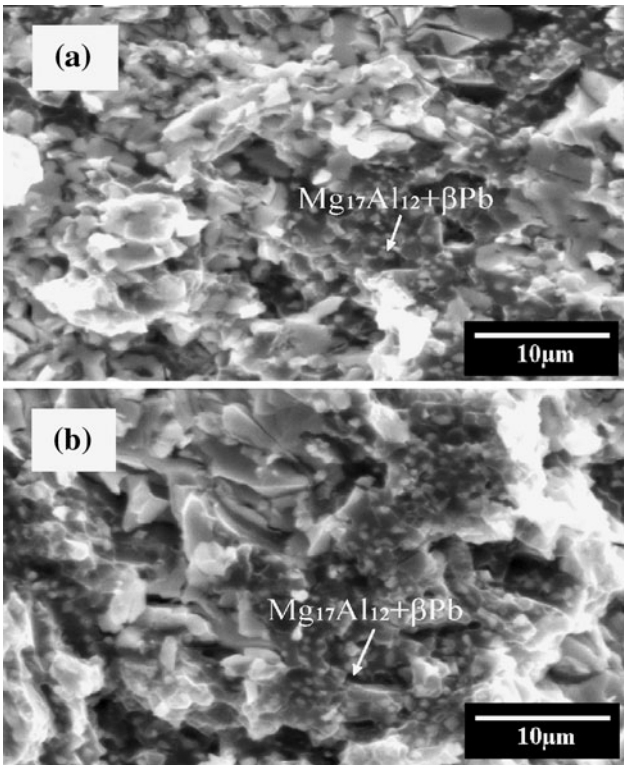

Fig. 3 SEM micrographs of the alloys 1 and 2 after failure: (a) the SEM image on fracture surface of alloy 1; (b) the SEM image on fracture surface of alloy 2

presents the intergranular quasi-cleavage morphology, the characteristic typical of brittle deformation. It establishes that the Pb-Mg-Al alloys' fractures are in the form of brittle fracture, and the fracture model changes from mixed intergranular-transgranular to the intergranular quasi-cleavage with the Al content increasing. These results confirm the experimental elongation results of Pb-Mg-Al alloys. Furthermore, there are very fine and dense phases as marked by arrows. The EDX analysis of these phases yield two atomic ratios among Mg, Al, and Pb of approximately 17:12:2 in alloy 1 and 17:12:0.8 in alloy 2, confirming the composition of these phases as $Mg_{17}Al_{12}$ and β-Pb phases.

4. Conclusions

1. Two typical Pb-Mg-Al alloys have been successfully prepared through casting. With the addition of Al content, the increasing nature of ultrafine acicular $Mg_{17}Al_{12}$ and β-Pb phase governs the growth of Mg_2Pb and eutectic α-Mg and Mg_2Pb. The average size of grain in Pb-Mg-Al alloys diminishes.
2. Accordingly, the Pb-Mg-Al alloys reveal high tensile strength and hardness values of 300 MPa and 156 HB, respectively, with obviously lower plastic strains reaching 0.68%. However, the values of the strength in the Pb-Mg-Al alloys in the present investigations are much higher than that of the conventional Pb matrix alloys, i.e., ~40 MPa, indicating that the Pb-Mg-Al alloys have potential to be utilized as engineering and structure materials of choice with higher strength.
3. The fractographic examinations indicate that the fracture model of Pb-Mg-Al alloys changes from mixed intergranular-transgranular to the intergranular quasi-cleavage with the increase of Al content.

Acknowledgments

The study was supported by the National Natural Science Foundation of China under Grant no. 50871049, and the National High-Tech Research and Development Program of China (863 Program) under Grant no. 2009AA03Z512.

References

1. T.P. Moseley, Lead/Acid Battery Myths, *J. Power Sources*, 1996, **59**, p 81–86
2. L.S.H. Yang, L. Liu, Y.H. Pan, and H.T. Ai, Performance of Pb-Sb-RE Alloys, *Chin. J. Power Sources*, 1995, **19**, p 15–18 (in Chinese)
3. S. Zhong, H.K. Liu, S.X. Dou, and M. Skyllas-Kazacos, Evaluation of Lead-Calcium-Tin-Aluminum Grid Alloys for Valve-Regulated Lead/Acid Batteries, *J. Power Sources*, 1996, **59**, p 123–129
4. Ch.T. Yu, *Metallic Matrix Composites*, 1st ed., Metallurgical Industry Press, Beijing, 1995, p 28–29 (in Chinese)
5. M.X. Tong and G.F. Lin, The Study of the Properties of the Lead-Based Grid Materials with Rear Earth Additive, *Phys. Test. Chem. Anal. A Phys. Test.*, 2006, **42**, p 60–63 (in Chinese)
6. Y.F. Yan, J.P. Liu, Y.W. Shi, and Z.H.D. Xia, Effect of Ag and Ni Fine Particles on Mechanical Properties of SnPb Composite Solder, *Rare Met. Mater. Eng.*, 2005, **34**, p 622–626 (in Chinese)
7. G. Cacciamani, G. Borzone, A. Saccone, and R. Ferro, Heat Content of Magnesium-Lead Alloys, *J. Less-Common Met.*, 1989, **154**, p 109–113
8. R.J. Wang and H.F. Zhao, Effect of Heat Treatment on Microstructure and Mechanical Properties of Mg-Pb Alloy, *Res. Stud. Foundry Equip.*, 2007, **2**, p 6–9 (in Chinese)
9. Q. Wang, Y.G. Chen, S.F. Xiao, H.M. Liu, Y.B. Tang, and Y.H. Zhao, Microstructures, Mechanical Properties and Compressive Creep Behaviors of As-Cast Mg-5%Sn-(0-1.0)%Pb Alloys, *J. Cent. South Univ. Technol.*, 2011, **18**, p 290–295
10. Y.H. Duan, Y. Sun, J. Feng, and M.J. Peng, Thermal Stability and Elastic Properties of Intermetallics Mg_2Pb, *Physica B*, 2010, **405**, p 701–704
11. Y.J. Liang, Y.C.H. Che, X.X. Liu, and N.J. Li, *Inorganic Thermodynamics Data Manual*, 1st ed., Northeast University Press, Shenyang, 1993, p 228 (in Chinese)
12. D.W. Zhou, P. Peng, H.L. Zhuang, Y.J. Hu, and J.S.H. Liu, First-Principle Study on Structural Stability of Ca Alloying $Mg_{17}Al_{12}$ Phase, *Chin. J. Nonferrous Met.*, 2005, **15**, p 546–551 (in Chinese)
13. C.H.M. Liu, X.Y. Zhu, and H.T. Zhou, *Magnesium Alloy Phase Diagrams*, 1st ed., Central South University Press, Changsha, 2006, p 132–134 (in Chinese)
14. S.R. Li, *Lead and Lead Alloys*, 1st ed., Central South China University of Technology Press, Changsha, 1996, p 26–38 (in Chinese)
15. S. Fouache, A. Chabrol, G. Fossati, M. Bassini, M.J. Sainz, and L. Atkins, Effect of Calcium, Tin and Silver Contents in the Positive Grids of Automotive Batteries With Respect to the Grid Manufacturing Process, *J. Power Sources*, 1999, **78**, p 12–22
16. K.M. Kumar, V. Kripesh, and A.A.O. Tay, Influence of Single-Wall Carbon Nanotube Addition on the Microstructural and Tensile Properties of Sn-Pb Solder Alloy, *J. Alloys Compd.*, 2008, **455**, p 148–158
17. Y.H. Duan, Y. Sun, M.J. Peng, L. Lu, and R.L. Zhao, Electronic Structure and Elastic Properties of Intermetallics Mg_2Pb, *Chin. J. Nonferrous Met.*, 2009, **19**, p 1835–1839 (in Chinese)
18. S.F. Pugh, Relations Between the Elastic Moduli and the Plastic Properties of Polycrystalline Pure Metals, *Philos. Mag.*, 1954, **45**, p 823–843